

HEMATOPOIESIS AND STEM CELLS

Perturbed hematopoiesis in mice lacking ATMIN

Fernando Anjos-Afonso,^{1,2} Joanna I. Loizou,^{3,4} Amy Bradburn,¹ Nnennaya Kanu,^{3,5} Sukhveer Purewal,⁶ Clive Da Costa,³ Dominique Bonnet,¹ and Axel Behrens^{3,7}

¹Haematopoietic Stem Cell Laboratory, The Francis Crick Institute, Lincoln's Inn Fields Laboratory, London, United Kingdom; ²Haematopoietic Signalling Group, European Cancer Stem Cell Research Institute, School of Biosciences, Cardiff University, Cardiff, United Kingdom; ³Mammalian Genetics Laboratory, The Francis Crick Institute, Lincoln's Inn Fields Laboratory, London, United Kingdom; ⁴Research Center for Molecular Medicine of the Austrian Academy of Sciences, Vienna, Austria; ⁵Translational Cancer Therapeutics Laboratory, UCL Cancer Institute, University College London, London, United Kingdom; ⁶Flow Cytometry Laboratory, The Francis Crick Institute, Lincoln's Inn Fields Laboratory, London, United Kingdom; and ⁷Diabetes & Nutritional Sciences Division, Faculty of Life Sciences & Medicine, King's College London, London, United Kingdom

Key Points

- ATMIN deletion using Vav-Cre causes chronic leukopenia, with fewer B cells and common myeloid progenitors.
- Long-term HSCs in ATMIN-deficient mice show increased cell cycling and are more prone to exhaustion under stress.

The ataxia telangiectasia mutated (ATM)-interacting protein ATMIN mediates non-canonical ATM signaling in response to oxidative and replicative stress conditions. Like ATM, ATMIN can function as a tumor suppressor in the hematopoietic system: deletion of *Atpin* under the control of CD19-Cre results in B-cell lymphomas in aging mice. ATM signaling is essential for lymphopoiesis and hematopoietic stem cell (HSC) function; however, little is known about the role of ATMIN in hematopoiesis. We thus sought to investigate whether the absence of ATMIN would affect primitive hematopoietic cells in an ATM-dependent or -independent manner. Apart from its role in B-cell development, we show that ATMIN has an ATM-independent function in the common myeloid progenitors (CMPs) by deletion of *Atpin* in the entire hematopoietic system using Vav-Cre. Despite the lack of lymphoma formation, ATMIN-deficient mice developed chronic leukopenia as a result of high levels of apoptosis in B cells and CMPs and induced a compensatory mechanism in which HSCs displayed enhanced cycling. Consequently, ATMIN-deficient

HSCs showed impaired regeneration ability with the induction of the DNA oxidative stress response, especially when aged. ATMIN, therefore, has multiple roles in different cell types, and its absence results in perturbed hematopoiesis, especially during stress conditions and aging. (*Blood*. 2016;128(16):2017-2021)

Introduction

Ataxia telangiectasia mutated (ATM) protein coordinates cell-cycle checkpoints with DNA repair in response to DNA damage.¹ ATM can be activated by the MRE11/RAD50/NBS1 complex via interaction with NBS1² but can also be activated by the ATM interactor ATMIN,³ also known as ASCIZ.⁴ ATMIN has a complementary function to NBS1: NBS1 is required for ionizing radiation-induced ATM signaling, whereas ATMIN is required for ATM activation after hypotonic or replication stress.^{3,5,6}

ATMIN has been shown to function in conditions of oxidative stress and aging⁷ and as a transcription factor.⁸ We have previously shown that ATMIN-deleted B cells (induced by CD19-Cre) have impaired class switch recombination and increased genomic instability, leading to B-cell lymphomas.⁹ In contrast, mice conditionally deleted of *Atpin* using Mx1-Cre developed B-cell lymphopenia.¹⁰ It is unclear whether the lack of B-cell lymphoma formation in this mouse model is due to a B-cell developmental defect or to other deficiencies in primitive hematopoietic cells that prevent the accumulation of genetically unstable cells. Because the role of ATMIN in hematopoietic stem/progenitor cells is currently unknown, we sought to investigate a possible role for ATMIN in primitive hematopoietic cells and whether this would be ATM-dependent or -independent.

Study design

Vav-Atmin^{Δ/Δ} mice

Atpin^{off} mice (described previously^{7,9}) were crossed with heterozygous Vav1-Cre (Vav-Cre) mice to generate Vav-*Atpin*^{Δ/Δ} mice. Gene deletion efficiency and genotyping was determined by polymerase chain reaction (PCR) using primers specific for floxed exon 4, deleted exon 4, or wild-type *Atpin* alleles, and Vav-Cre, as well as immunoblotting (see supplemental Figure 1A-B and supplemental Table 1, available on the *Blood* Web site).

Intracellular immunostaining

Briefly,¹¹ cells were incubated with antibodies against extracellular antigens, and then fixed in phosphate-buffered saline (PBS) with 2% methanol-free formaldehyde at room temperature (for Ki-67 [BD Biosciences]) or at 37°C (for pS824-Kap1 [Bethyl Laboratories], Bim [Cell Signaling], and pS139-γH2AX [Abcam]) for 10 minutes. Cells were permeabilized with PBS containing 0.1% Triton-X-100 (Sigma) for 10 minutes at room temperature, blocked using PBS containing 5% serum for 15 minutes, and incubated with primary antibodies at 4°C for 1 hour, followed by appropriate secondary antibodies in the same conditions. Cells were resuspended with PBS/2% fetal bovine serum containing

Submitted 30 September 2015; accepted 25 August 2016. Prepublished online as *Blood* First Edition paper, 31 August 2016; DOI 10.1182/blood-2015-09-672980.

The online version of this article contains a data supplement.

The publication costs of this article were defrayed in part by page charge payment. Therefore, and solely to indicate this fact, this article is hereby marked "advertisement" in accordance with 18 USC section 1734.

© 2016 by The American Society of Hematology

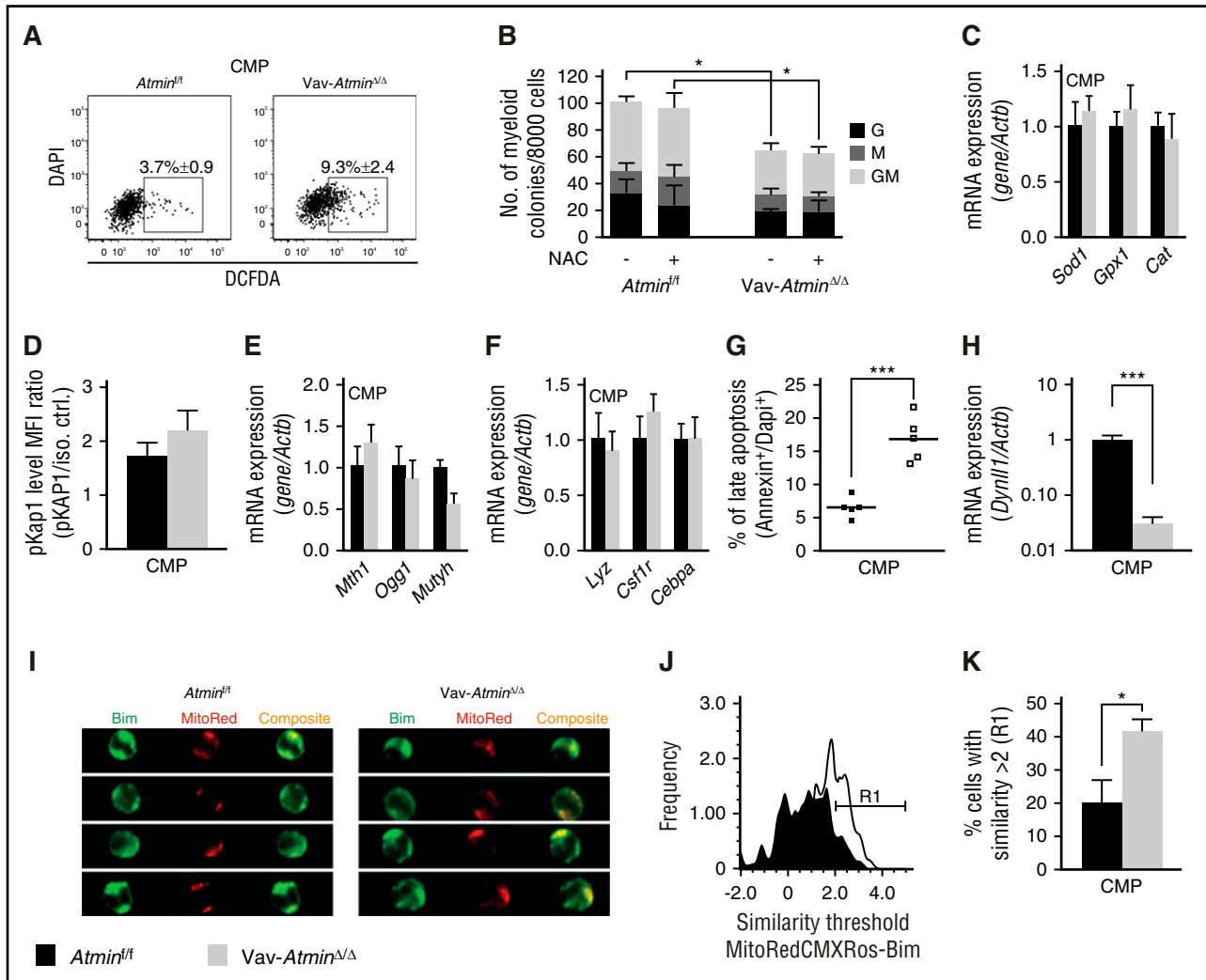


Figure 1. ATMIN-deficient mice have a reduced CMP compartment due to increased apoptosis. Black bars/symbols represent *Atmin*^{fl/fl}, and open symbols/gray bars represent *Vav-Atmin*^{Δ/Δ}, unless otherwise indicated. (A) Dichlorodihydrofluorescein diacetate (DCFDA) stains for ROS detection showing a mild increase in the percentage of ROS-positive cells in ATMIN-deficient CMPs (n = 3/genotype). (B) Treating total BM cells with the antioxidants *N*-acetylcysteine (NAC) or γ -glutamylcysteinylethyl ester (not shown) was unable to rescue the myeloid colony formation defect of *Vav-Atmin*^{Δ/Δ} cells (n = 5/genotype). (C) Expression of key antioxidant genes was unchanged between ATMIN-deficient and control CMPs. Expression values were determined by qRT-PCR and were relative to the mean (n = 3-5/genotype). (D-F) In ATMIN-deficient CMPs compared with control CMPs, no significant increase in pKap1 levels (indicative of ATM activation) (D), upregulation of genes required for DNA oxidation repair (E), or changes in the indicated CMP developmental factors (F) were detected. pKap1 levels were determined by intracellular flow cytometry analysis (mean fluorescence intensity [MFI] ratios are shown), and qRT-PCR was used to determine the expression of the indicated genes (n = 5-6/genotype). The frequency of late apoptosis was significantly increased (G) and *Dynll1* expression was drastically reduced (H) in CMPs lacking ATMIN compared with control cells (n = 4-6/genotype). (I) Representative cell images captured by an ImageStream flow cytometer in green and red channels, followed by their respective composite images, showing higher colocalization of mitochondria (red) with Bim (green) staining in *Vav-Atmin*^{Δ/Δ} CMPs. (J) Representative MitoTrackerRed-CMXRox and Bim similarity staining score histograms for *Atmin*^{fl/fl}-derived (black) and *Vav-Atmin*^{Δ/Δ}-derived (open) CMPs respectively. A score above value 2 (R1) indicates translocation of Bim into mitochondria. (K) Percentage of Bim translocation in CMPs (n = 3/genotype). The different BM hematopoietic stem and progenitor populations were defined as follows: LT-HSC, Lineage⁻Sca-1⁺cKit⁺ (L⁻S⁺K⁺)CD34⁻Flt3⁻; short-term HSC, L⁻S⁺K⁺CD34⁺Flt3⁺; multipotent progenitor, L⁻S⁻K⁺CD34⁺Flt3⁺; CMP, L⁻S⁻K⁺IL7R⁻CD34⁺Fc γ R⁻; granulocyte (G) monocyte (M) progenitor, L⁻S⁻K⁺IL7R⁻CD34⁺Fc γ R⁺; megakaryocyte-erythroid progenitor, L⁻S⁻K⁺IL7R⁻CD34⁻Fc γ R⁻; and common lymphoid progenitor, L⁻S⁻K⁺IL7R⁺. Mean and standard deviation values are shown. **P* < .03; ****P* < .0003. DAPI, 4',6-diamidino-2-phenylindole; HSC, hematopoietic stem cell; LT, long-term; mRNA, messenger RNA; qRT, quantitative reverse transcription.

4',6-diamidino-2-phenylindole, and pulse processing was used to exclude any unstained, apoptotic, and clumped cells.

Please see supplemental Methods for more details.

Results and discussion

Vav-Atmin^{Δ/Δ} mice were born healthy and were not anemic but were leukopenic at 8 to 12 weeks (supplemental Figure 1C-D). Unlike the CD19-Cre model,⁹ mice did not develop lymphoma (even aged mice);

instead, numbers of splenic B cells were reduced (supplemental Figure 2A-B), which resulted in a complete absence of germinal centers (supplemental Figure 2C). B-cell apoptosis was increased, and although reactive oxygen species (ROS) levels were unaffected, there was a pronounced reduction in *Dynll1* expression, as previously described¹⁰ (supplemental Figure 2D-F). In addition, ATMIN-deficient B cells displayed a significant increase in DNA damage signaling, consistent with an ATM-dependent competitive function of ATMIN^{3,5} (supplemental Figure 2G-H). Numbers of pre-B cells in the bone marrow (BM) were also significantly lower (supplemental Figure 2I-K). These data suggest an early developmental defect with a concomitant

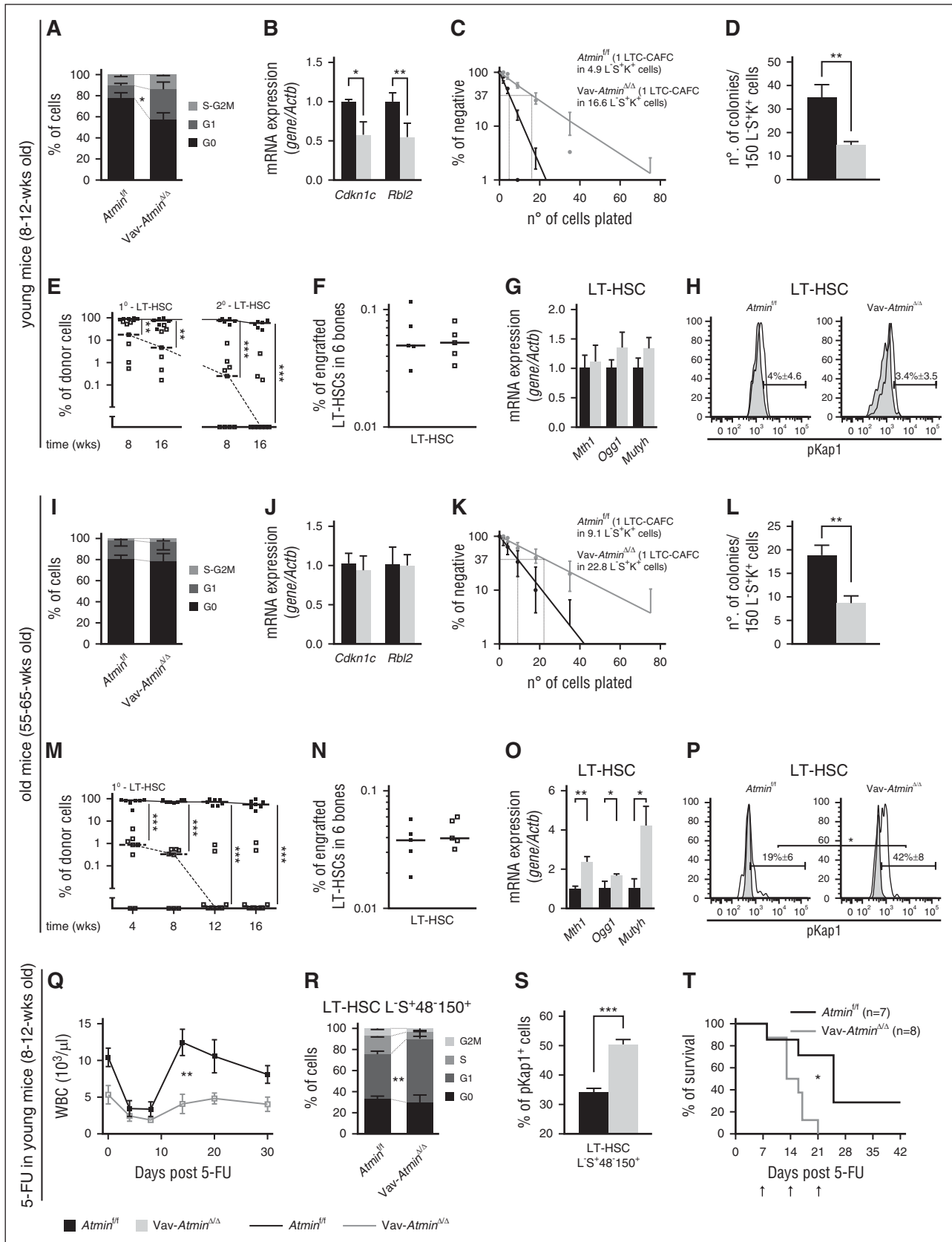


Figure 2. Vav-Atmin $\Delta\Delta$ LT-HSCs have impaired functions during regeneration and aging. Experiments were performed with young (A-H and Q-T) and aged (I-P) BM cells. Black bars/symbols and lines represent *Atmin*^{fl}, and open symbols/gray bars and lines represent *Vav-Atmin* ^{$\Delta\Delta$} , unless otherwise indicated. (A,I) Cell cycle distribution was determined using Ki67/DAPI stains in BM LT-HSCs (n = 4/genotype). (B, J) qRT-PCR for the expression of *Cdkn1c* and *Rbl2* in LT-HSCs. Expression values are relative to the mean of control (n = 3-5/genotype). Other cell cycle regulators were unchanged between ATMIN-deficient and control cells (data not shown). (C,K) To estimate the stem/progenitor cell capacity of the more primitive cells, the frequency of L⁻S⁺K⁺ cells to form CAFCs was determined by limiting dilution 5 weeks after seeding on MS5 stroma. (D,L) Five-week LT culture-initiating cell-derived

high level of apoptosis that does not allow the accumulation of damaged B cells in the Mx1-Cre model¹⁰ and the *Vav-Atmin*^{ΔΔ} mice. We then analyzed the primitive hematopoietic cell compartment in more detail.

In young ATMIN-deficient mice (8-12 weeks), an ~40% reduction in BM cellularity was observed across all cell types, with a prominent reduction in the frequency of common myeloid progenitors (CMPs) (supplemental Figure 3A-B). The very modest oxidative stress detected in the CMPs did not seem to play an evident role in reducing this cellular fraction in ATMIN-deficient mice (Figure 1A-C). We observed neither an increased DNA damage response (Figure 1D-E) nor evidence of developmental defects (Figure 1F) in *Vav-Atmin*^{ΔΔ} CMPs compared with control cells. However, a significant increase in late apoptosis was detected in *Vav-Atmin*^{ΔΔ} CMPs (Figure 1G), but not in other primitive compartments (data not shown), and this was accompanied by an ~33-fold decrease in *Dynll1* expression (a direct transcriptional target of ATMIN⁸; Figure 1H). Because Dynll1 sequesters pro-apoptotic Bim away from mitochondria,¹² reduced Dynll1 levels in *Vav-Atmin*^{ΔΔ} CMPs should free Bim to translocate to mitochondria, triggering higher apoptosis. Consistent with this, immunofluorescence revealed significant co-staining of Bim with MitoTracker dye in *Vav-Atmin*^{ΔΔ} cells (Figure 1I-K).

Because two major cell compartments downstream of LT-HSCs were severely affected, we hypothesized that LT-HSC function could be compromised. Indeed, subpopulations upstream of CMPs, particularly LT-HSCs, consisted of more cells that had exited quiescence (Figure 2A; supplemental Figure 3C), supported by reduced expression of *Cdkn1c* (*p57^{Kip2}*) and *Rbl2* (p130) (Figure 2B). In addition, ATMIN-deficient primitive cells had a two- to threefold reduction in the frequency of cobblestone area-forming cells (CAFCs) and LT culture-initiating cell-derived colonies compared with control cells (Figure 2C-D). Importantly, the regenerative capacity of *Vav-Atmin*^{ΔΔ} LT-HSCs 16 weeks posttransplantation was reduced 16-fold compared with control cells, affecting all 3 lineages (Figure 2E; supplemental Figure 3D), and this was not due to homing defects (Figure 2F). *Vav-Atmin*^{ΔΔ} LT-HSCs were mostly unable to regenerate hematopoiesis when retransplanted (Figure 2E), despite the apparent lack of oxidative stress, increased apoptosis (supplemental Figure 3E-F), or active DNA damage response in young *Vav-Atmin*^{ΔΔ} cells at steady state (Figure 2G-H). These results suggest that stresses induced during regeneration disturbed LT-HSC function.

Consistent with disturbed LT-HSC function, aged (55- to 65-week-old) *Vav-Atmin*^{ΔΔ} mice continued to have reduced BM cellularity (supplemental Figure 3G), with similar defects in aged ATMIN-deficient B cells as reported⁹ (data not shown), as well as a reduced CMP compartment (supplemental Figure 3H). Although the numbers of short-term HSCs and multipotent progenitors were not altered in aged ATMIN-deficient mice, the proportion of these

subpopulations was increased, perhaps due to increased cell cycling in younger, but not in aged, mice (Figure 2I-J; supplemental Figure 3H-I). As in young mice, ATMIN-deficient primitive cells from aged mice had a reduced capacity to produce CAFCs and LT culture-initiating cell colonies (Figure 2K-L), and LT-HSCs lacking ATMIN were unable to provide long-term reconstitution (Figure 2M), although BM homing was unaffected (Figure 2N). There were no apparent signs of senescence (such as increased *p16^{Ink4a}* and *p19^{Arf}* expression) in any of the aged ATMIN-deficient primitive subpopulations (data not shown), and no increase in ROS production in ATMIN-deficient LT-HSCs was observed (supplemental Figure 3J), unlike in *Atm*^{-/-} mice.^{13,14} Contrary to young cells, we observed a significant increase in expression of DNA oxidation repair genes in aged ATMIN-deficient LT-HSCs, as well as an increase in pKap1, suggesting that both aging and ATMIN deficiency are required to stimulate this response (Figure 2O-P). Regeneration of peripheral blood hematopoiesis after myelosuppressive 5-fluorouracil (5-FU) treatment was much weaker in ATMIN-deficient mice compared with control mice (Figure 2Q). ATMIN-deficient LT-HSCs cycled less and showed an increase in ATM signaling response compared with control cells at day 7 post-5-FU treatment (Figure 2R-S). *Vav-Atmin*^{ΔΔ} mice succumbed to multiple doses of 5-FU faster than *Atmin*^{fl/fl} mice (Figure 2T).

We reveal ATMIN as a novel player with multiple functions in hematopoiesis. These functions are both ATM-dependent and -independent. We have uncovered a novel and important ATM-independent function of ATMIN in the CMP compartment. ATMIN-deficient mice also have impaired LT-HSC function during regeneration and aging, most likely due to exhaustion from compensating for the reduced/damaged lymphoid and myeloid compartments over time. It would be interesting to dissect other possible roles that ATMIN might have in myeloid development using more specific lineage gene deletion approaches, because myeloid cells can differentiate without passing the CMP stage.¹⁵⁻¹⁷

Acknowledgments

The authors thank the Biological Resources Unit and Flow Cytometry core facility for valuable technical help and C. Cremona for help with manuscript editing.

This work was supported by The Francis Crick Institute, which receives its core funding from Cancer Research UK (FC001045 and FC001039), the Medical Research Council (FC001045 and FC001039), and the Wellcome Trust (FC001045 and FC001039). This work was also supported by a European Research Council grant (281661 ATMINDDR) (A. Behrens).

Figure 2 (continued) colonies were also determined (n = 3/genotype). (E,M) To evaluate the regeneration capacity of LT-HSCs, peripheral blood (PB) chimerism was determined at different time points from sublethally irradiated NSG (nonobese diabetic/severe combined immunodeficiency disease/interleukin-2 receptor γ -chain-null) mice; CD45.1 due to the mixed background) that were transplanted with 15 LT-HSCs from either (E) young or (M) aged *Atmin*^{fl/fl} or *Vav-Atmin*^{ΔΔ} mice (CD45.2). After 16 weeks, 15 LT-HSCs were sorted by flow cytometry from primary mice and retransplanted into separate secondary recipients, and PB chimerism was determined at different time points. (F,N) Percentage of engrafted LT-HSCs 16 hours after IV injection of total *Atmin*^{fl/fl} or *Vav-Atmin*^{ΔΔ} BM mononuclear cells (n = 2 independent experiments). Each symbol indicates a mouse, and horizontal lines represent median reconstitution levels. (G,O) qRT-PCR for the expression of the indicated DNA oxidation repair genes in LT-HSCs was also evaluated. Expression values were relative to the mean of each control subpopulation (n = 3/genotype). (H, P) pKap1 expression in LT-HSCs was determined by intracellular flow cytometry analysis. Gray and open histograms represent isotype-matched control and pKap1 stains, respectively (n = 3/genotype). (Q) Hematopoietic reconstitution was monitored by serial PB counts in mice injected with a single dose of 5-FU. Total white blood cell (WBC) counts are shown (n = 5-6/genotype). Cell cycle status (R) and pKap1 expression (S) in ATMIN-deficient and control LT-HSCs at day 7 after a single dose of 5-FU administration (n = 4-5/genotype). (T) Kaplan-Meier survival curve of *Atmin*^{fl/fl} and *Vav-Atmin*^{ΔΔ} mice injected 3 times (arrows) with 5-FU (n = 7-8/genotype). Unless stated, mean and standard deviation values are shown. **P* < .03; ***P* < .003; ****P* < .0003.

Authorship

Contribution: F.A.-A. conceived, designed, and performed the experiments and wrote the manuscript; J.I.L. provided mice and conceived and performed some experiments; A. Bradburn performed some experiments; S.P. optimized, performed, and analyzed the data related to ImageStream experiments; N.K. provided mice and helped design experiments; C.D.C.: maintained and rederived the mouse colony; and D.B. and A. Behrens conceived the study.

Conflict-of-interest disclosure: The authors declare no competing financial interests.

Correspondence: Axel Behrens, Mammalian Genetics Laboratory, The Francis Crick Institute, Lincoln's Inn Fields Laboratory, 44 Lincoln's Inn Fields, London WC2A 3LY, United Kingdom; e-mail: axel.behrens@crick.ac.uk; and Dominique Bonnet, Haematopoietic Stem Cell Laboratory, The Francis Crick Institute, Lincoln's Inn Fields Laboratory, 44 Lincoln's Inn Fields, London WC2A 3LY, United Kingdom; e-mail: dominique.bonnet@crick.ac.uk.

References

- Shiloh Y, Ziv Y. The ATM protein kinase: regulating the cellular response to genotoxic stress, and more. *Nat Rev Mol Cell Biol*. 2013; 14(4):197-210.
- Uziel T, Lerenthal Y, Moyal L, Andegeko Y, Mittelman L, Shiloh Y. Requirement of the MRN complex for ATM activation by DNA damage. *EMBO J*. 2003;22(20):5612-5621.
- Kanu N, Behrens A. ATMIN defines an NBS1-independent pathway of ATM signalling. *EMBO J*. 2007;26(12):2933-2941.
- McNees CJ, Conlan LA, Tennis N, Heierhorst J. ASCIZ regulates lesion-specific Rad51 focus formation and apoptosis after methylating DNA damage. *EMBO J*. 2005;24(13):2447-2457.
- Zhang T, Penicud K, Bruhn C, et al. Competition between NBS1 and ATMIN controls ATM signaling pathway choice. *Cell Reports*. 2012; 2(6):1498-1504.
- Kanu N, Zhang T, Burrell RA, et al. RAD18, WRNIP1 and ATMIN promote ATM signalling in response to replication stress. *Oncogene*. 2016; 35(30):4009-4019.
- Kanu N, Penicud K, Hristova M, et al. The ATM cofactor ATMIN protects against oxidative stress and accumulation of DNA damage in the aging brain. *J Biol Chem*. 2010;285(49):38534-38542.
- Jurado S, Conlan LA, Baker EK, et al. ATM substrate Chk2-interacting Zn²⁺ finger (ASCIZ) is a bi-functional transcriptional activator and feedback sensor in the regulation of dynein light chain (DYNLL1) expression. *J Biol Chem*. 2012; 287(5):3156-3164.
- Loizou JI, Sancho R, Kanu N, et al. ATMIN is required for maintenance of genomic stability and suppression of B cell lymphoma. *Cancer Cell*. 2011;19(5):587-600.
- Jurado S, Gleeson K, O'Donnell K, et al. The Zinc-finger protein ASCIZ regulates B cell development via DYNLL1 and Bim. *J Exp Med*. 2012;209(9): 1629-1639.
- Anjos-Afonso F, Currie E, Palmer HG, Foster KE, Taussig DC, Bonnet D. CD34(-) cells at the apex of the human hematopoietic stem cell hierarchy have distinctive cellular and molecular signatures. *Cell Stem Cell*. 2013;13(2):161-174.
- Puthalakath H, Huang DC, O'Reilly LA, King SM, Strasser A. The proapoptotic activity of the Bcl-2 family member Bim is regulated by interaction with the dynein motor complex. *Mol Cell*. 1999; 3(3):287-296.
- Ito K, Hirao A, Arai F, et al. Regulation of oxidative stress by ATM is required for self-renewal of haematopoietic stem cells. *Nature*. 2004; 431(7011):997-1002.
- Ito K, Takubo K, Arai F, et al. Regulation of reactive oxygen species by Atm is essential for proper response to DNA double-strand breaks in lymphocytes. *J Immunol*. 2007;178(1):103-110.
- Adolfsson J, Månsson R, Buza-Vidas N, et al. Identification of Flk3+ lympho-myeloid stem cells lacking erythro-megakaryocytic potential a revised road map for adult blood lineage commitment. *Cell*. 2005;121(2):295-306.
- Arinobu Y, Mizuno S, Chong Y, et al. Reciprocal activation of GATA-1 and PU.1 marks initial specification of hematopoietic stem cells into myeloerythroid and myelolymphoid lineages. *Cell Stem Cell*. 2007;1(4):416-427.
- Pronk CJ, Rossi DJ, Månsson R, et al. Elucidation of the phenotypic, functional, and molecular topography of a myeloerythroid progenitor cell hierarchy. *Cell Stem Cell*. 2007;1(4):428-442.